Tricyclic antipsychotics and antidepressants can inhibit α5-containing GABA$_A$ receptors by two distinct mechanisms

Konstantina Bampali (1), Filip Koniuszewski (1), Luca L. Silva (1), Sabah Rehman (2), Florian D. Vogel (1), Thomas Seidel (3), Petra Scholze (1), Florian Zirpel (1), Arthur Garon (3), Thierry Langer (3), Matthäus Willeit (4), Margot Ernst* (1)

(1) Department of Pathobiology of the Nervous System, Center for Brain Research, Medical University Vienna, Spitalgasse 4, 1090 Vienna, Austria

(2) Department of Molecular Neurosciences, Center for Brain Research, Medical University of Vienna, Spitalgasse 4, 1090 Vienna, Austria

(3) Department of Pharmaceutical Sciences, Division of Pharmaceutical Chemistry, University of Vienna, Althanstraße 14, 1090 Vienna, Austria

(4) Department of Psychiatry and Psychotherapy, Medical University of Vienna, Währinger Gürtel 18-20, 1090, Vienna, Austria

*Corresponding author: margot.ernst@meduniwien.ac.at, phone number: +43 1 40160 34065

Running Title: Inhibition of GABA$_A$ receptors by antipsychotics and antidepressants

Abstract

Background and Purpose: Many psychotherapeutic drugs, including clozapine, display polypharmacology and act on GABA$_A$ receptors. Patients with schizophrenia show alterations in function, structure and molecular composition of the hippocampus, and a recent study demonstrated aberrant levels of hippocampal α5 subunit-containing GABA$_A$ receptors. The purpose of this study is to investigate tricyclic compounds in α5 subunit-containing receptor subtypes.

Experimental Approach: Functional studies of effects by seven antipsychotic and antidepressant medications were performed in several GABA$_A$ receptor subtypes by two-electrode voltage-clamp electrophysiology using *Xenopus laevis* oocytes. Computational structural analysis was employed to design mutated constructs of the α5 subunit, probing a novel binding site. Radioligand displacement data complemented the functional and mutational findings.

Key Results: We show that the antipsychotic drugs clozapine and chlorpromazine exert functional inhibition on multiple GABA$_A$ receptor subtypes, including α5-containing ones. Based on a chlorpromazine binding site observed in a GABA-gated bacterial homologue, we identified a novel site in α5 GABA$_A$ receptor subunits and demonstrate differential usage of this and the orthosteric sites by these ligands.

Conclusion and Implications: Despite high molecular and functional similarities among the tested ligands, they reduce GABA currents by differential usage of allosteric and orthosteric sites. The CPZ site we describe here is a new potential target for optimizing antipsychotic medications with beneficial polypharmacology. Further studies in defined subtypes are needed to substantiate mechanistic links between the therapeutic effects of clozapine and its action on certain GABA$_A$ receptor subtypes.

Keywords: GABA$_A$ receptor, clozapine, chlorpromazine, antipsychotics, allosteric modulation, functional inhibition

Abbreviations: positron emission tomography (PET), clozapine (CLZ), chlorpromazine (CPZ), loxapine (LOX) LOX, clotiapine (CLOT), imipramine (IMI), nortriptyline (NOR), levomepromazine (LEVO), negative allosteric modulation (NAM), bicuculline (BIC), [35S]t-butylbicyclophosphorothionate (TBPS), *Erwinia* ligand-gated ion channel (ELIC), γ-aminobutyric acid type A (GABA$_A$), Protein Data Bank (PDB), extracellular domain (ECD)

Bullet point summary

What is already known:

- Clozapine and other tricyclic molecules reduce GABA effects at ionotropic GABA receptors
- Chlorpromazine interacts with a novel site in a GABA-gated bacterial homologue

What this study adds:

- Clozapine's effects on $\alpha5\beta3\gamma2$ receptors are consistent with orthosteric antagonism
- Chlorpromazine does not displace [3H]muscimol, and interacts with a novel site in $\alpha5$ subunits

Clinical significance:

- Clozapine and chemically related molecules reduce GABA effects by two or more mechanisms
- $\alpha5$ subunit-dependent current inhibition might contribute to clinically observed drug effects

Introduction

Hippocampal dysfunction has long been considered to contribute to the pathophysiology of schizophrenia[1-3]. Post-mortem studies in the brains of patients with schizophrenia suggest that hippocampal and prefrontal expression of GABA$_A$ receptors is altered in a subtype-selective manner[4]. The $\alpha5$ GABA$_A$ receptor subunit, which is characterized by its relatively limited distribution and high abundance in the hippocampus, has thus been in the focus of clinical and preclinical schizophrenia research[5,6]. A recent positron emission tomography (PET) study using [11C]Ro15-4513, a radiotracer with high affinity to $\alpha5$-containing GABA$_A$ receptor subtypes, found evidence for aberrant receptor levels in the hippocampus of patients with schizophrenia[5]. Moreover, the study demonstrated a direct relationship between the expression of schizophrenia symptoms and hippocampal binding of [11C]Ro15-4513. The quest for $\alpha5$-containing subtype-preferring ligands has provided a number of compounds widely used in research[7-9]. These molecules exert allosteric modulatory effects that can range from GABA-induced current enhancement or reduction to silent but competitive binding[10]. Based on genetic and pharmacological studies, drugs which target $\alpha5$-containing GABA$_A$ receptors have been under investigation as cognitive enhancers[6]. Negative modulation of $\alpha5$-containing GABA$_A$ receptors has been shown to promote hippocampal gamma oscillations, long-term potentiation, and learning, as well as have antidepressant effects associated with restored synaptic strength in the form of increased glutamatergic excitatory activity[6,11,12]. Among the most recent developments was a clinical trial examining basmisanil, a compound exerting negative modulatory effects at $\alpha5$-containing GABA$_A$ receptors, as an add-on treatment for antipsychotic therapy aiming to alleviate cognitive impairment of patients with schizophrenia (https://clinicaltrials.gov/ct2/show/NCT02953639).

Not only GABA$_A$ receptor targeting drugs such as benzodiazepines or sedative general anesthetics elicit effects at these receptors by allosteric interaction sites, but a wide range of small molecules have been identified as GABA$_A$

receptor modulators, including multiple antipsychotic and antidepressant medications not intentionally targeting these receptors[13,14]. One of those is clozapine (CLZ), a tetracyclic compound displaying relatively weak dopamine receptor antagonism. However, it shows outstanding antipsychotic efficacy and ameliorates negative and cognitive symptoms of schizophrenia without inducing unwanted extrapyramidal side effects[15,16]. On the other hand, the effects of many antipsychotics, like chlorpromazine (CPZ), were mainly attributed to blockade of dopamine receptors and it has received only minor attention in terms of its effects on GABA_A receptors[17-20]. In the 80's and 90's, the interactions of several antipsychotics with GABA_A receptors have been considered serious candidates for eliciting part of the therapeutic effects, but were never studied in $\alpha5$-containing receptors[13,14,21-23].

There is broad consensus that CLZ can reduce GABA elicited effects by direct interactions with GABA_A receptors. The mechanism remains unclear and the binding sites were never identified[22,24-26]. In this work, we bridge this historical gap and examine the functional effects of CLZ and six chemically similar compounds in recombinantly expressed GABA_A receptors, including $\alpha5$-containing receptors. We demonstrate functional inhibition of GABA elicited currents. To further elucidate the molecular substrate of the observed effects, we investigate a novel intrasubunit binding site in the extracellular domain (ECD) of the $\alpha5$ subunit, which has been described as a CPZ site in the homologous GABA-gated *Erwinia* ligand-gated ion channel (ELIC)[27]. Accordingly, we find CPZ to inhibit α5-containing GABA_A receptors allosterically, but CLZ to be an orthosteric antagonist of this subtype.

Results

Functional profiles of CLZ and CPZ on different GABA_A receptor subtypes

First, we examined CLZ and CPZ effects on recombinantly expressed GABA_A receptors. We performed functional testing of the drugs' effects in a panel of subunit combinations with emphasis on subtypes discussed in the literature as candidate targets for alleviating some schizophrenia symptoms, namely $\alpha2$ and $\alpha5$ subunit-containing GABA_A receptors[6]. In earlier experiments where a different subtype panel was investigated, inhibitory as well as biphasic modulation of radioligand binding was observed[24], prompting us to use a low GABA concentration (EC_{5-10}) for the initial functional assessment. Only current reduction was seen in the tested range CLZ 1-100μM, no enhancement or biphasic effects (Figure 1a). Inhibition in the tested $\alpha1$-containing assemblies was less pronounced compared to $\alpha2$- and $\alpha5$-containing assemblies (Figure 1a, Supplementary Figure S1a, b). Additionally, the $\alpha5\beta3$ dose response curve was right shifted compared to $\alpha5\beta3\gamma2$ (Figure 1b, c). The current reduction approaches plateau at around 100μM for five subunit combinations, namely $\alpha1\beta2\gamma2$, $\alpha2\beta3$, $\alpha2\beta3\gamma2$, $\alpha2\beta3\gamma1$ and $\alpha5\beta3\gamma2$, but the extent of inhibition varied from 69% to 15% (Figure 1a, Supplementary Figure S1a). CPZ displays similar action as CLZ in $\alpha5\beta3\gamma2$ and $\alpha5\beta3$, and screening at 100μM in $\alpha1\beta3$ and $\alpha2\beta3$ revealed weaker current inhibition compared to CLZ (Figure 1d, e). Both compounds fail to inhibit currents in $\alpha3\beta3$ (Figure 1d, Supplementary Figure S1b).
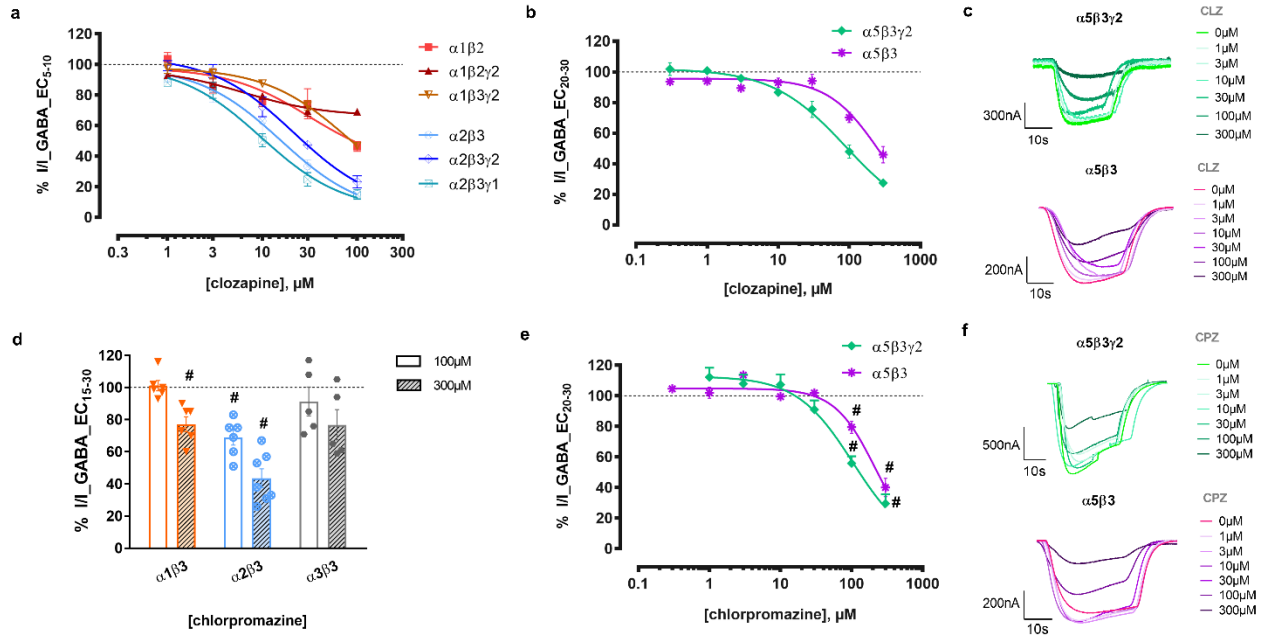
Figure 1. Functional inhibition of CLZ and CPZ on different GABA$_A$ receptor subtypes. (**a**) CLZ dose response effects elicited by an EC$_{5-10}$ GABA concentration in $\alpha 1\beta 2$ (n=5), $\alpha 1\beta 2\gamma 2$ (n=5-7), $\alpha 1\beta 3\gamma 2$ (n=6-9), $\alpha 2\beta 3$ (n=5-11), $\alpha 2\beta 3\gamma 2$ (n=6) and $\alpha 2\beta 3\gamma 1$ (n=5) receptors. The effects we observed by co-application of 100µM CLZ with GABA EC$_{5-10}$ are summarized in Supplementary Figure S1 (including effects on the additional subtype $\alpha 1\beta 3$). Data were fitted to the Hill equation using non-linear regression (fixed slope of 1) and points are depicted as mean ± SEM. Representative traces can be found in Supplementary Figure S2. (**b, e**) CLZ (**b**) and CPZ (**e**) dose response effects elicited by an EC$_{20-30}$ GABA concentration in $\alpha 5\beta 3\gamma 2$ receptors (n=5-11 and n=7-13) and in $\alpha 5\beta 3$ receptors (n=5-6 and n=6). Data were fitted to the Hill equation using non-linear regression (fixed bottom of 0) and points are depicted as mean ± SEM. (**c, f**) Representative traces from electrophysiological recordings of CLZ (**c**) and CPZ (**f**) co-applied with GABA in $\alpha 5\beta 3\gamma 2$ and $\alpha 5\beta 3$ receptors, corresponding to panels (**b**) and (**e**). The dotted line is used to visualize the baseline (100%) of control current. Tables reporting the IC$_{50}$, logIC$_{50}$, Hill slope and maximum efficacy values corresponding to panels (**a**), (**b**) and (**e**) can be found in Supplementary Tables S1, S2 and S3. (**d**) Modulation of currents elicited by an EC$_{15-30}$ GABA concentration by 100µM and 300µM CPZ in $\alpha 1\beta 3$ (n=6 and n=6), $\alpha 2\beta 3$ (n=6 and n=7) and $\alpha 3\beta 3$ (n=5 and n=5) receptors. One sample t test was performed to determine statistical significance of each mean response from control current and corrected for multiple comparisons using the false discovery rate method of Benjamini and Hochberg, with a discovery rate of 0.05 (#p<0.05). The response with 100µM in $\alpha 2\beta 3$, $\alpha 5\beta 3$ and $\alpha 5\beta 3\gamma 2$ receptors was significantly different from control, while with 300µM the responses in $\alpha 1\beta 3$, $\alpha 2\beta 3$, $\alpha 5\beta 3$ and $\alpha 5\beta 3\gamma 2$ receptors were significant from control (#p<0.05 - panels d and e).

Neurosteroids, like THDOC, have been shown to directly activate GABA$_A$ receptors[28]. We also examined whether CLZ could inhibit neurosteroid-activated currents, similarly to known orthosteric antagonists[29]. Here, CLZ does not inhibit THDOC-gated currents in $\alpha 1\beta 3$ GABA$_A$ receptors (Supplementary Figure S1c). Moreover, in an effort to assess the impact of the alpha subunit on the observed effects, we compared CLZ responses between $\alpha 5\beta 2\gamma 2$ and $\beta 2\gamma 2$ receptors. The latter receptors have been previously described and were found to be GABA-gated, as well as modulated by diazepam and etomidate[30]. Removal of the $\alpha 5$ subunit from the receptor assembly eliminates a significant part of the effect (Supplementary Figure S1d). CPZ is completely inactive in $\beta 2\gamma 2$ receptors (Supplementary Figure S1e). Similar to the diversity of effects observed in a [35S]TBPS modulation study[24], each subunit isoform influences the net effect of clozapine on a given subunit combination.

Investigation of additional tricyclic compounds

Different studies accumulated over the years showed CLZ and several other antipsychotic and antidepressant drugs to fully or partially inhibit GABA$_A$ receptors[13,14,22,23,31]. Most of the prior work was done in membrane preparations

from rodent brains. We, therefore, chose to test a selection of compounds that were already investigated by Squires and Saederup in the 80s and 90s but in defined recombinantly expressed subunit combinations. Additional tricyclic compounds with comparable chemical structures to CLZ were tested, namely levomepromazine, imipramine, nortriptyline, loxapine and clotiapine (LEVO, IMI, NOR, LOX and CLOT; Figure 2a).

All of these compounds share a cyclic scaffold composed of two benzene rings flanking a central, non-aromatic 6- or 7-membered ring with a substituent that carries a terminal amino group. For a more in-depth investigation of structural and stereoelectronic similarities between the selected compounds we performed pairwise shape alignments using the software ROCS[32]. Three types of scores were computed and analyzed further, namely pure shape similarity (shape), overlap of shared features (color), and a combination score (combo) which considers both shape and feature overlap. 2D scatter plots of the compounds via a multidimensional scaling procedure of the similarity scores visualize the calculated scores of each compound pair (Figure 2b, Supplementary Figure S4). The visual analysis of the scatter plots revealed two groups, namely CPZ, IMI, NOR, LEVO and LOX, CLOT, CLZ (Figure 2b). For a more in-depth investigation of ligand similarities in terms of common chemical features and the resulting receptor interaction capabilities, we generated ligand-based pharmacophore models for both ligand groups using the software LigandScout[33,34]. The group comprising CPZ-LEVO-IMI-NOR has two hydrophobic, two aromatic and one positive ionizable feature (Figure 2c). LOX and CLOT contain several additional features, while CLZ shares with LOX and CLOT three hydrophobic, two aromatic, one positive ionizable and one halogen bonding feature, where not all can be aligned simultaneously (Figure 2c, Supplementary Figure S5). All drugs have two hydrophobic, one aromatic and one positive ionizable feature in common. The overall shape similarity is high across all seven compounds, and thus suggestive of shared targets while differences in features may reflect in some non-overlapping targets.
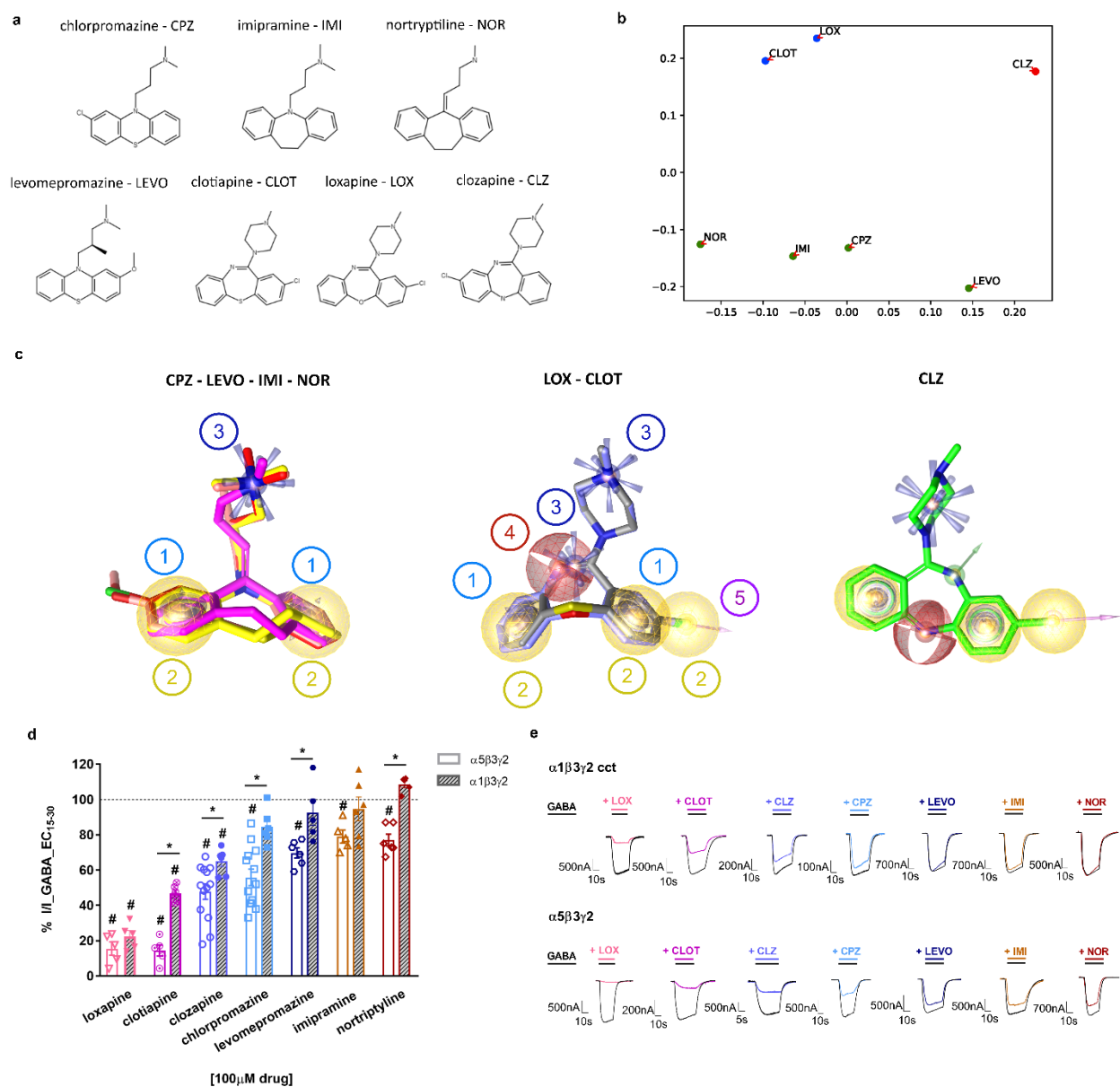
Figure 2. Chemical structures and selected properties of all drugs investigated in this study. (**a**) Chemical structures of clozapine, chlorpromazine, levomepromazine, imipramine, nortriptyline, loxapine and clotiapine (and their abbreviations). (**b**) 2D scatter plot of the compounds where the proximity of the points correlates with the corresponding Tanimoto Combo similarity scores calculated by ROCS and the axes reflect a dimensionless distance. Supplementary Figures S3, S4 show the raw data and the results of hierarchical clustering. Individual shape, color and combo scores can be found in Supplementary Table S4. (**c**) Ligand-based shared feature pharmacophores generated by LigandScout of the ligand groups that emerged from panel b. Features: 1 – aromatic (blue donuts), 2 – hydrophobic (yellow spheres), 3 – positive ionizable (blue stars/rays), 4 – hydrogen bond acceptor (red sphere), 5 – halogen bond donor (magenta arrow). (**d**) Modulation of currents elicited by an EC_{15-30} GABA concentration by 100μM CLZ (n=13), CPZ (n=13), NOR (n=6), IMI (n=5), LEVO (n=6), LOX (n=5) and CLOT (n=5) in $\alpha5\beta3\gamma2$ and in concatenated $\alpha1\beta3\gamma2$ wild-type receptors (n=6, n=6, n=5, n=6, n=5, n=5, n=6, respectively). Subset of data in $\alpha5\beta3\gamma2$ receptors for CLZ from Figure 1d, reproduced here for the comparison with $\alpha1\beta3\gamma2$ receptors. Columns for each receptor subtype depict mean ± SEM. Statistically significant differences were determined for each compound between $\alpha5\beta3\gamma2$ and $\alpha1\beta3\gamma2$ receptors by two-tailed students t-test and corrected for multiple comparisons using the false discovery rate method of Benjamini and Hochberg, with a discovery rate of 0.05 (*p<0.05). Additionally, one sample t test was performed for each subtype separately to determine statistical significance of each mean response from control current and was also corrected for multiple comparisons using the false discovery rate method of Benjamini and Hochberg, with a

6

discovery rate of 0.05 ($^{\#}p<0.05$). The mean response in $\alpha 1\beta 3\gamma 2$ receptors was not significantly different from control current for CPZ, LEVO, IMI and NOR. The mean response in $\alpha 5\beta 3\gamma 2$ receptors was significantly different from control current for all drugs. (**e**) Representative traces from electrophysiological recordings of LOX, CLOT, CLZ, CPZ, LEVO, IMI and NOR co-applied with GABA in $\alpha 1\beta 3\gamma 2$ (concatenated) and $\alpha 5\beta 3\gamma 2$ receptors.

While all these compounds (except LEVO) have been shown to interact with GABA$_A$ receptors, their functional effects have never been compared systematically. We thus, examined their effects on GABA currents in $\alpha 1\beta 3\gamma 2$ (concatenated[35]) and $\alpha 5\beta 3\gamma 2$ receptors (Figure 2d, e). All of them diminish GABA elicited currents in $\alpha 5\beta 3\gamma 2$ receptors, and all but LOX and IMI elicit greater peak current inhibition in the $\alpha 5$-containing subtype. The CPZ-LEVO-IMI-NOR group has no significant effect in the $\alpha 1\beta 3\gamma 2$ receptor at 100µM.

Computational exploration of candidate binding sites

GABA elicited currents can be reduced by multiple different mechanisms, specifically by direct pore block at the picrotoxin site, by competitive antagonism at the orthosteric site akin to bicuculline (BIC), and by negative allosteric modulation from different allosteric sites such as the Bz-site, for which a gamma subunit is needed (Figure 3a). The observation that CLZ and CPZ do not need the gamma subunit for effective reduction of GABA currents rules out the Bz-site for their action, in line with previous work[24].

We turned to structural data from the Protein Data Bank (PDB) in order to perform a computational exploration of the remaining candidate binding sites. GABA$_A$ receptor structures in picrotoxin and BIC bound states are available[36,37]. In a search for homologous proteins in complex with any of our test ligands, a CPZ bound structure of a homologous, bacterial GABA-gated pentameric channel, namely ELIC[28] was found. The CPZ pocket observed in the bacterial superfamily member has been previously suggested to be compatible with homology models of GABA$_A$ receptors[38], where it is located near the disulfide bridge in the packing core between the ECD inner and outer sheets.

First, we performed a pharmacophore-based screening of the investigated compounds using structure-based pharmacophores generated for picrotoxin and BIC bound states of GABA$_A$ receptors and the CPZ bound ELIC (Figure 3c). The screening runs were performed at two different levels of stringency: a) all features have to be matched and b) one feature may be omitted to obtain a match. No matches were found for the pharmacophore of the picrotoxin site at high stringency, and CPZ matched with one omitted feature. For the BIC/GABA site all ligands match in the stringent screening run, and for the CPZ site in ELIC, LOX, CPZ, CLOT match in the stringent run while the remaining ligands match with less stringent settings. Due to these results, we moved on to further explore the CPZ site and the orthosteric site. As alpha subunits strongly influence the net effect elicited by CPZ or CLZ, we chose to investigate the novel candidate CPZ site in the $\alpha 5$ subunit taking advantage of a recently published cryo-EM structure of $\alpha 5\beta 3$ (Figure 3d)[39].
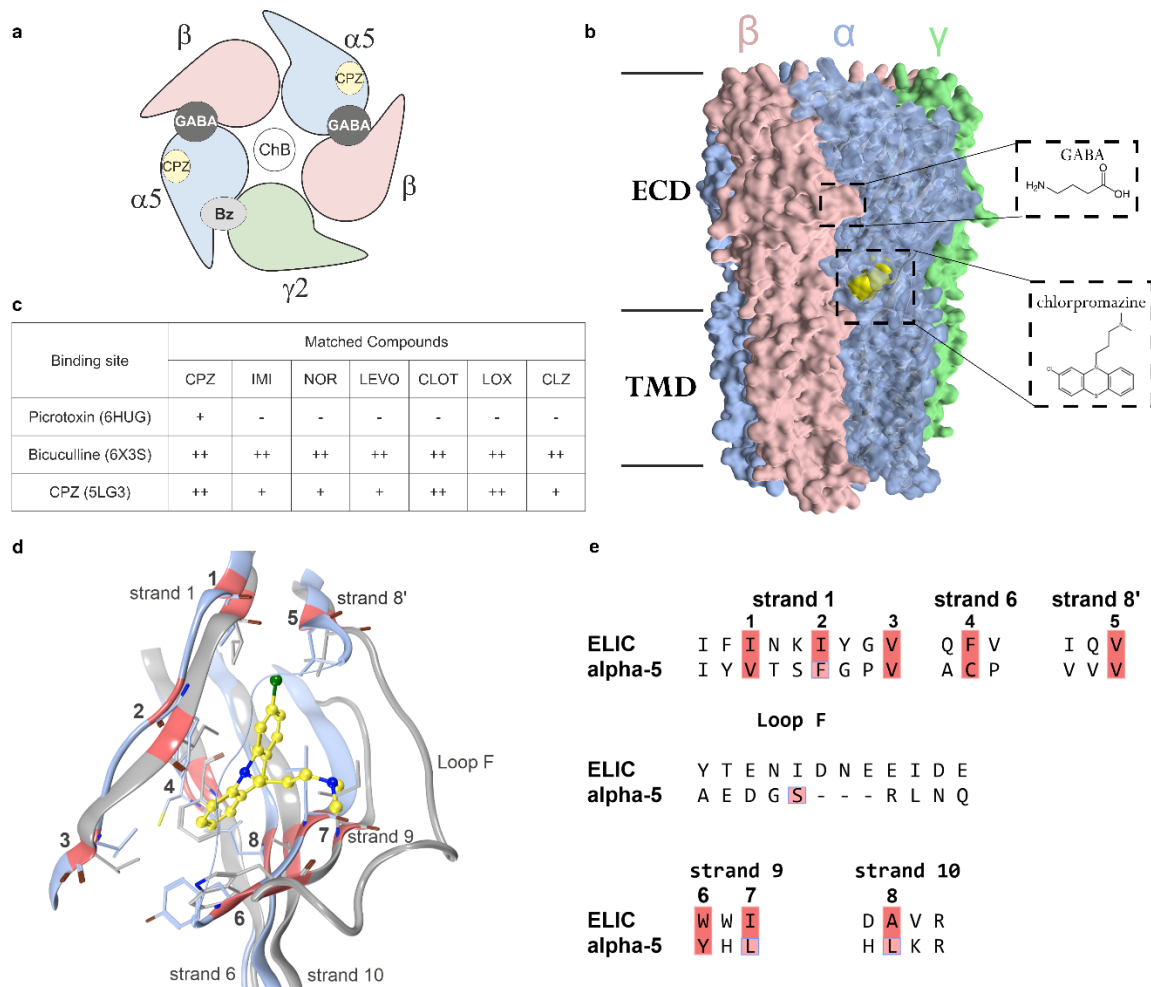
Figure 3. Candidate binding sites for the current reduction elicited by the tricyclic compounds and the putative CPZ pocket in the α5 subunit. (**a**) Cartoon view of a receptor with the canonical subunit arrangement, the pointed side of the subunit is the principal side. The localization of the GABA/ bicuculline sites (orthosteric sites) and the high affinity Bz-sites are at subunit interfaces. The Channel blocker (ChB) site is localized in the pore domain. The candidate site for CPZ in the α5 subunit is depicted as yellow circle, the alpha subunit in blue, beta in red and gamma in green. (**b**) Space filling representation of a heteropentameric GABA_A receptor (PDB ID: 6A96) with CPZ docked into the candidate binding site in yellow space filling representation. The insets display GABA and CPZ structures and binding site localizations. Sequences with binding site forming amino acids and a comparison among alpha isoforms are provided in Supplementary Figure S6. (**c**) Table of the pharmacophore screening results into the selected bound state structures: ++ = all features matched, + = match with one omitted feature, - = no match. (**d**) Homology between the CPZ site in ELIC (5LG3) and the corresponding pocket in the α5 subunit of 6A96. 3D superposition of an α5 (light blue) subunit of 6A96 and ELIC (5LG3 in grey), respectively. Strands 1, 6 and 10 are highly conserved, and the hydrophobic amino acids forming the large deep portion of the pocket overlap closely, while loop F is longer in ELIC. (**e**) Partial sequence alignment of the pocket forming protein segments of ELIC with the GABA_A receptor α5 subunit. The hydrophobic pocket core positions are highlighted red and correspond with the red ribbon markings in panel (**d**). The amino acids highlighted in pink boxes indicate sites chosen for mutational analysis (Figure 4a).

The binding site occupied by CPZ in ELIC[27] is formed by hydrophobic sidechains located on strands 1, 6 and 10 and capped by the backside of segment (loop) F, which provides both hydrophobic and polar interactions. CPZ interacts with the pocket mainly via van der Waals contacts of the tricyclic core, while the sidechain forms polar interactions with hydrophilic groups of segment F[27]. Superposition with the available structure of the α5 subunit indicates good overlap of the strands, and very little overlap for the segment F (Figure 3d).

**Mutational analysis of the putative CPZ binding site in the α5 subunit**

Encouraged by the good superposition of the CPZ bound structure and the α5 subunit, four mutations in the α5 subunit were chosen based on pocket forming residues and their proximity to the ligand (Figure 4a). Tryptophane residues were introduced individually into the four sites and in one double mutant in order to diminish the pocket volume (Figure 4a, b).

In subsequent experiments, each α5 subunit mutant was co-expressed individually with β3 and γ2, forming α5(mut)β3γ2 receptors. The GABA dose response curves of α5F53Wβ3γ2, α5L222Wβ3γ2 as well as α5F53W;L122Wβ3γ2 were matching the wild-type, in comparison to the other two that were right-shifted (Figure 5c). Diazepam effects (1μM) were also examined in all mutated receptors and were above ~200% in wild-type and mutated receptors, which ensures the incorporation of the γ2 subunit (Figure 4d). The known Bz-site negative modulator DMCM was used as an additional control for unspecific effects of the mutants in α5F53Wβ3γ2, α5L222Wβ3γ2 as well as α5F53W;L122Wβ3γ2. Only the double mutant displays a small but significant alteration in the DMCM modulation (Figure 4e). Effects of the individual mutations on current reduction by 100μM CPZ were significant for α5L222Wβ3γ2 and α5F53W;L122Wβ3γ2, and none induced significant changes for CLZ (Figure 4f, g). The most informative mutant was α5L222Wβ3γ2, with normal responses to GABA, diazepam and DMCM. Thus, the α5L222W mutant and the double mutant α5F53W;L122W were used to screen all our compounds for change in effect (Figure 4h-l). More specifically, LOX, CLOT and CLZ are not influenced by either mutant, while for CPZ, LEVO, IMI and NOR the inhibition is reduced by both mutants (Figure 4f, g and h-l).

a

b

c

- ○— α5β3γ2
- ◆— α5L222Wβ3γ2
- ☐— α5F53Wβ3γ2
- △— α5F53W;L222Wb3g2
- ○— α5L196Wβ3γ2
- ▽— α5S189Wβ3γ2

d

[1μM diazepam]

e

[200nM DMCM]

[GABA]

f

[chlorpromazine]

g

[clozapine]

h

[100μM imipramine]

i

[100μM nortriptyline]

j

[100μM levomepromazine]

k

[100μM loxapine]

l

[100μM clotiapine]

10
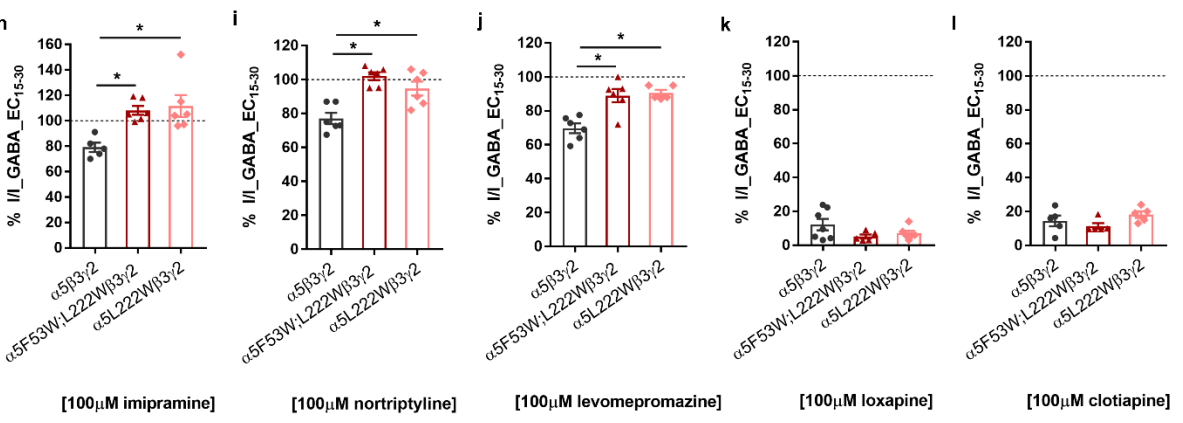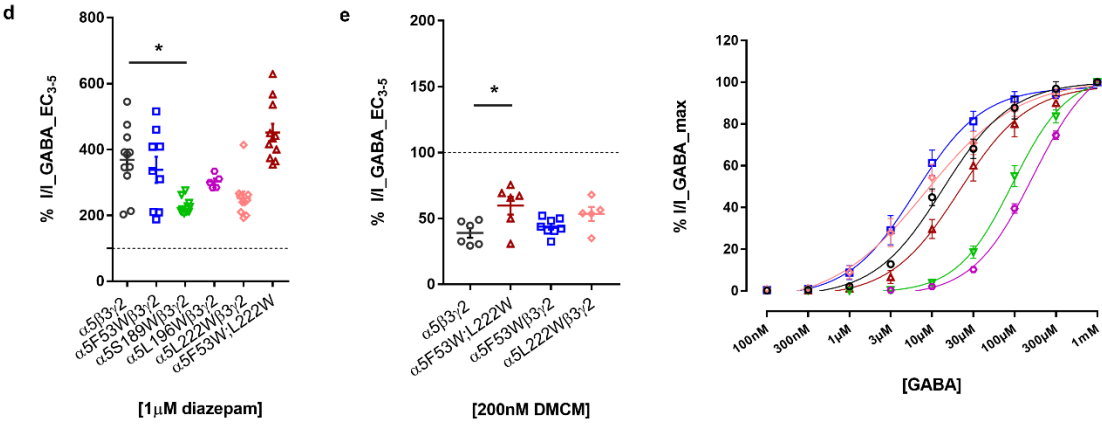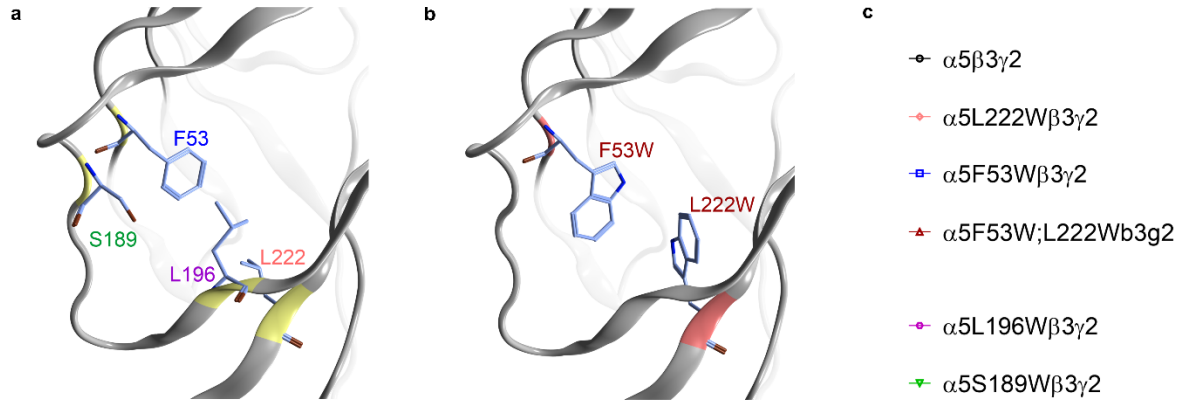
Figure 4. Mutational analysis of the putative binding site in the α5 subunit impacts on some of the drugs' effects. (**a**) Binding site region of the α5 subunit of the GABA$_A$ receptor, highlighting the residues subjected to mutational analysis, namely F53, S189, L196 and L222 where the colour codes of the labels match panel c. (**b**) Structural rendering of F53W;L222W. The estimated volume of the binding site is reduced in the double mutant by up to 46%, depending on rotameric states. (**c**) GABA dose response curves in α5β3γ2 (n=5), α5F53Wβ3γ2 (n=6), α5S189Wβ3γ2 (n=6), α5L196Wβ3γ2 (n=6), α5L222Wβ3γ2 (n=6) and α5F53W;L222Wβ3γ2 (n=5) receptors. Data were normalized and fitted to the Hill equation using non-linear regression and points are depicted as mean ± SEM. Tables reporting the EC$_{50}$, logEC$_{50}$, Hill slope and amplitude at 1mM values can be found in Supplementary Table S5. (**d, e**) Modulation of currents elicited by an EC$_{3-5}$ GABA concentration by 1μM diazepam (**d**) and 200nM DMCM (**e**) in α5β3γ2 (n=11 and n=6), α5F53Wβ3γ2 (n=9 and n=8), α5S189Wβ3γ2 (n=9), α5L196Wβ3γ2 (n=5), α5L222Wβ3γ2 (n=10 and n=5) and α5F53W;L222Wβ3γ2 (n=11 and n=6) receptors. Sufficient positive allosteric modulation by 1μM diazepam and negative allosteric modulation by 200nM DMCM was achieved for all tested cells (≥200% and ≤50%, respectively). Columns depict mean ± SEM. Statistically significant differences were determined for DMCM between mutated and wild-type receptors by one-way ANOVA followed by Dunnett's multiple comparisons test, where *p<0.05. For diazepam statistically significant differences were determined by non-parametric one-way ANOVA (Kruskal-Wallis test) followed by Dunn's multiple comparisons test, where *p<0.05. (**f, g**) Modulation of currents elicited by an EC$_{15-30}$ GABA concentration by 30 and 100μM CPZ (**f**), as well as by 30 and 100μM CLZ (**g**) in α5β3γ2 wild-type (n=13 for 100μM CPZ and n=13 for 100μM CLZ, n=11 for 30μM CPZ and n=10 for 30μM CLZ), α5F53Wβ3γ2 (n=13 for 100uM CPZ and n=11 for 100μM CLZ, n=13 for 30μM CPZ and n=11 for 30μM CLZ), α5S189Wβ3γ2 (n=6 for 100μM CPZ and n=6 for 100μM CLZ, n=6 for 30μM CPZ and n=6 for 30μM CLZ), α5L196Wβ3γ2 (n=5 for 100μM CPZ and n=5 for 100μM CLZ, n=5 for 30μM CPZ and n=6 for 30μM CLZ), α5L222Wβ3γ2 (n=11 for 100μM CPZ and n=11 for 100μM CLZ, n=11 for 30μM CPZ and n=11 for 30μM CLZ) and α5F53W;L222Wβ3γ2 (n=14 for 100μM CPZ and n=10 for 100μM CLZ, n=10 for 30μM CPZ and n=11 for 30μM CLZ) mutated receptors. Columns for each receptor subtype depict mean ± SEM. Statistically significant differences were determined for each compound between mutated and wild-type receptors by non-parametric one-way ANOVA (Kruskal-Wallis test) followed by Dunn's multiple comparisons test, where *p<0.05. (**h-l**) Modulation of currents elicited by an EC$_{15-30}$ GABA concentration by 100μM IMI (n=6) (**h**), NOR (n=6) (**i**), LEVO (n=6) (**j**), LOX (n=5) (**k**) and CLOT (n=5) (**l**) in α5F53W;L222Wβ3γ2 and by 100μM IMI (n=6) (**h**), NOR (n=6) (**i**), LEVO (n=5) (**j**), LOX (n=6) (**k**) and CLOT (n=5) (**l**) in α5L222Wβ3γ2 mutated receptors, compared to α5β3γ2 wild-type receptors,. All drug effects in wild-type receptors as in Figure 2d are reproduced for direct comparison. Columns depict mean ± SEM. Statistically significant differences were determined for each compound between mutated and wild-type receptors by one-way ANOVA followed by Dunnett's multiple comparisons test, where *p<0.05. In order to ascertain that we don't overlook differences for LOX and CLOT at compound concentrations that elicit a lower degree of inhibition, we repeated the experiments at additional compound concentrations and also saw no effect of the double mutant (Supplementary Figure S8).

As the α5L222W mutant and the double mutant α5F53W;L122W impacted on the CPZ effect, but data for CLZ were inconclusive, we investigated our compounds of major interest - CLZ and CPZ - over a compound concentration range (Figure 5a-f, Supplementary Figure S9). The α5F53W mutation did not influence the IC$_{50}$ of either compound (Supplementary Figure S9). None of the mutants impacted on the IC$_{50}$ of CLZ (Figure 5a, b, c), while the IC$_{50}$ of CPZ functional inhibition was right shifted in α5L222Wβ3γ2 and in the double mutant α5F53W;L122Wβ3γ2 (Figure 5d, e, f).
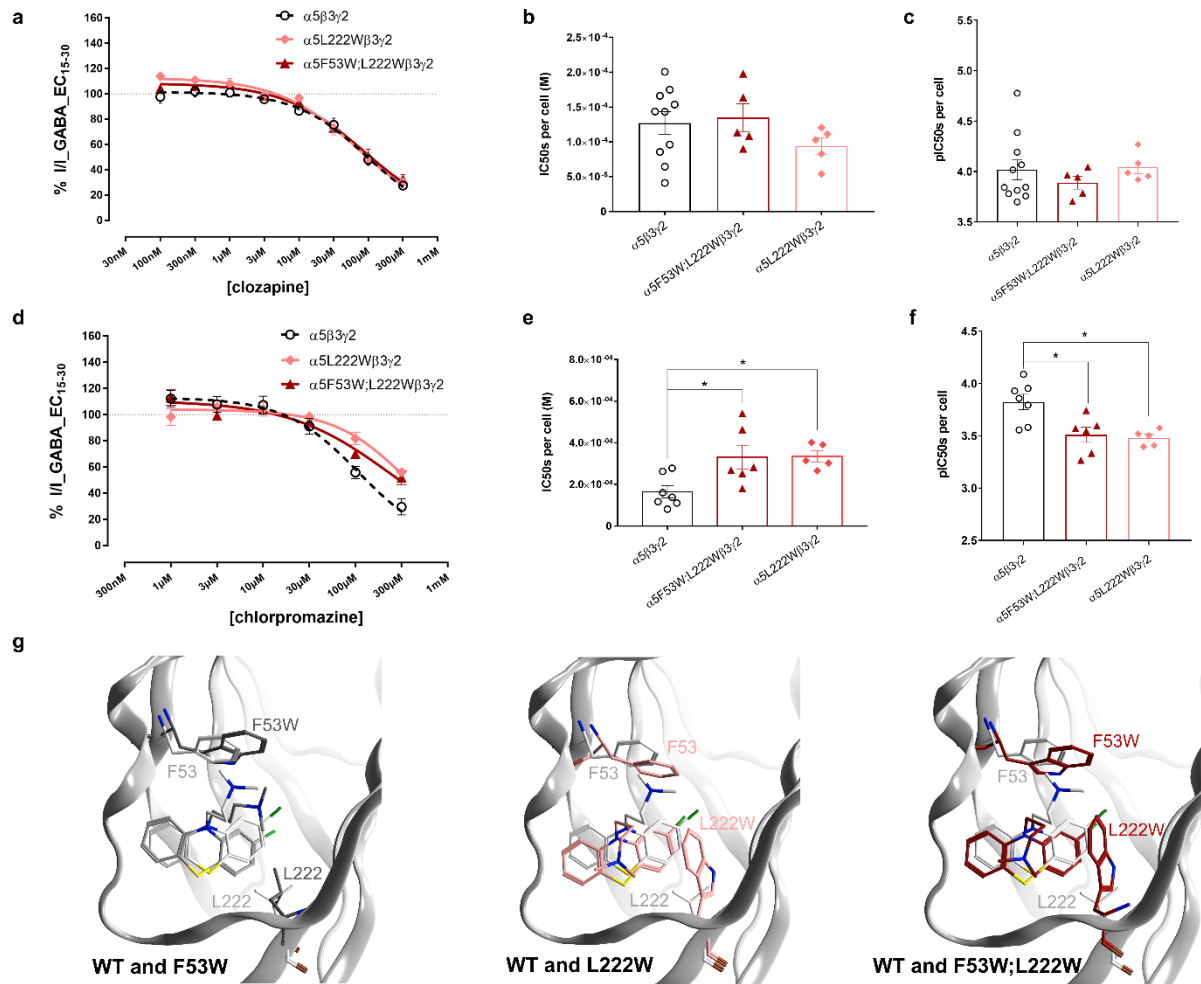
Figure 5. Mutational analysis of the putative binding site in the α5 subunit impacts on CPZ effects, but not CLZ. (**a**, **d**) CLZ (**a**) and CPZ (**d**) dose response curves in α5β3γ2, α5L222Wβ3γ2 and α5F53W;L222Wβ3γ2 receptors (α5F53Wβ3γ2 receptors in Supplementary Figure S9). Data were normalized and fitted to the Hill equation using non-linear regression (fixed bottom of 0) and points are depicted as mean ± SEM. The precise n numbers, as well as the IC_{50}, $logIC_{50}$, Hill slope and maximum efficacy values can be found in Supplementary Tables S6 and S7. Dose response curves in α5β3γ2 receptors are represented with dotted lines, as they are also depicted in Figures 1 and reproduced here for easier comparisons. (**b, e**) The column graphs depict the IC_{50} values for CLZ (**b**) and CPZ (**e**) dose response effects in α5β3γ2, α5L222Wβ3γ2 and α5F53W;L222Wβ3γ2 receptors by fitting data of each cell individually. (**c, f**) The column graphs depict the pIC_{50} values for CLZ (**c**) and CPZ (**f**) dose response effects in α5β3γ2, α5L222Wβ3γ2 and α5F53W;L222Wβ3γ2 receptors by fitting data of each cell individually. Statistically significant differences were determined for each compound between mutated and wild-type receptors by one-way ANOVA followed by Dunnett's multiple comparisons test, where *p<0.05. (**g**) Representative, energy minimized molecular docking poses of CPZ in α5β3γ2 (white), α5F53Wβ3γ2 (grey), α5L222Wβ3γ2 (pink) and α5F53W;L222Wβ3γ2 (red) receptors.

The impact of the double mutant was expected to be stronger based on pocket volume computation, prompting a more detailed follow up on a possible structural hypothesis for the small change in IC_{50}. Docking of CPZ into the four investigated pockets (wild-type and the three mutants depicted in Figure 5g) resulted in several good candidate binding modes based on consensus scoring (see methods and Supplementary Figure S10). Thus, docking suggests that CPZ can be accommodated by the pocket in the wild type and the mutated pockets. The structural hypothesis which is most in line with no effect of the α5F53W mutant and an equal right shift for α5L222W and the double mutant α5F53W;L122W is displayed in Figure 5g. Other candidate binding modes including one that is similar to the 5LG3 structure are in Supplementary Figure S10, along with their putative interaction features. In total, the data

from the computational and mutational analysis suggests that a CPZ site homologous to the one described in ELIC exists in the $\alpha 5$ subunit of GABA$_A$ receptors.

Investigation of orthosteric site usage

The structure-based pharmacophore screening suggested the BIC site as a candidate for all seven compounds (Figure 3c, Supplementary Figure S11a). In order to investigate whether CLZ or CPZ inhibition in the recombinant $\alpha 5\beta 3\gamma 2$ receptors might be elicited by orthosteric competition, we compared their inhibition at GABA ~EC$_5$ and ~EC$_{20}$ (Figure 6a-d). This comparison is indicative of a right shift for CLZ and thus with a partly or fully competitive mode of action for CLZ. On the other hand, and in line with an allosteric effect, there is no significant change in pIC$_{50}$ values for CPZ between GABA ~EC$_5$ and ~EC$_{20}$ (Figure 6c, d).
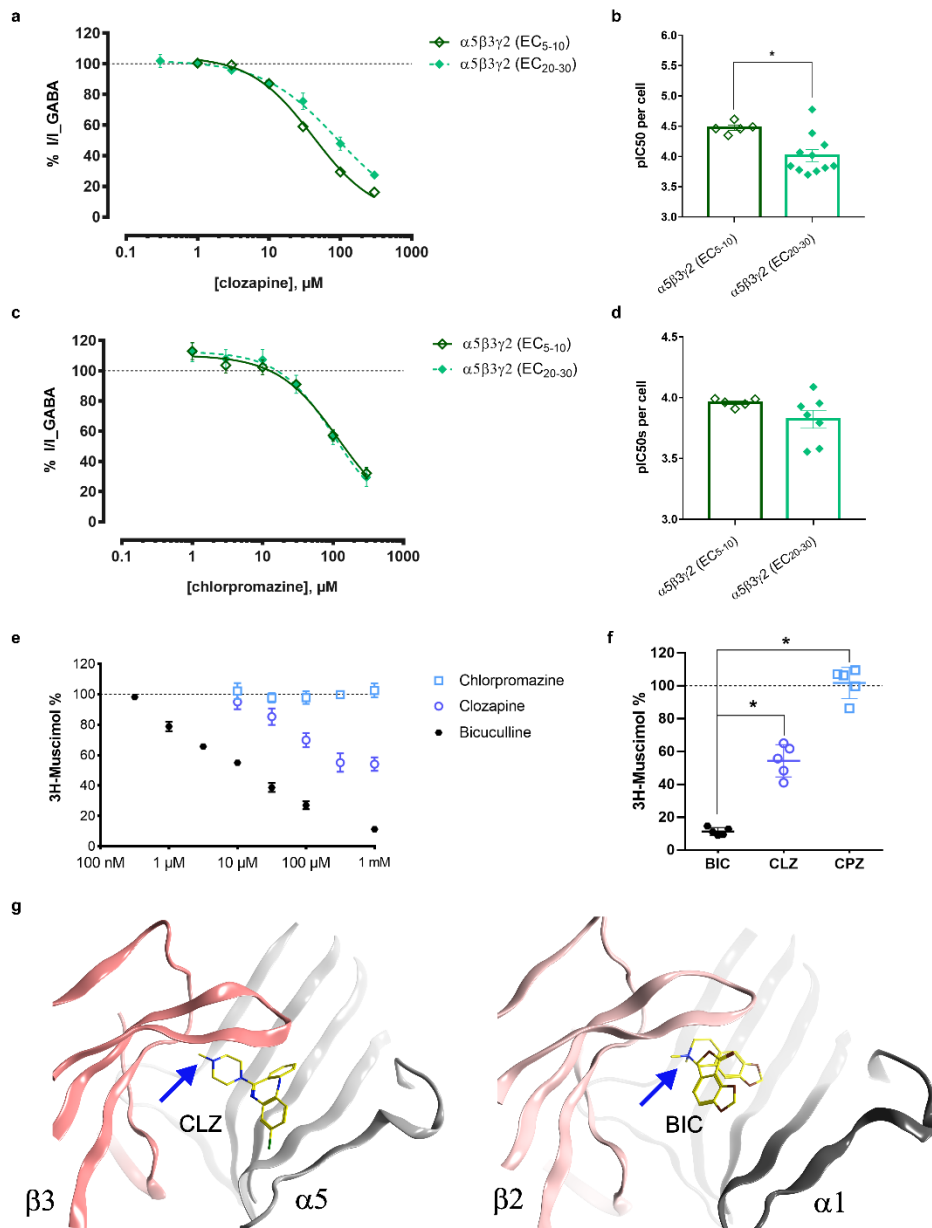
Figure 6. **Exploration of orthosteric site usage by CLZ and CPZ.** (**a, c**) CLZ (**a**) and CPZ (**c**) dose response effects elicited by an EC_{20-30} and an EC_{5-10} GABA concentration in $\alpha5\beta3\gamma2$ receptors. Data were fitted to the Hill equation using non-linear regression (fixed bottom of 0) and points are depicted as mean ± SEM. (**b, d**) The column graphs depict the pIC_{50} values for CLZ (**b**) and CPZ (**d**) dose response effects at EC_{5-10} (n=5 and n=5) and EC_{20-30} (n=11 and n=7) GABA concentration in $\alpha5\beta3\gamma2$ receptors by fitting data of each cell individually. Statistically significant differences were determined by two-tailed students t-test, where *p<0.05. The dotted line is used to visualize the baseline (100%) of control current. Tables reporting the IC_{50}, $logIC_{50}$, Hill slope and maximum efficacy values corresponding to panels (d) and (f) can be found in Supplementary Tables S2 and S3. (**e**) Inhibition of binding of [3H]muscimol to rat hippocampal membrane GABA$_A$ receptors (n=3-5). Membranes were incubated with 10nM [3H]muscimol in the presence of various concentrations of the displacing ligand. 100% is the amount of radioligand bound in the presence of 1% DMSO. Data shown are mean ± SEM of three independent experiments performed in duplicates each (for the concentrations <1mM) and five independent experiments performed in duplicates each (for 1mM). Visual inspection and sigmoid fitting indicated that the displacement points are not described by a single sigmoid function, as would be expected due to different affinities for the diversity of subtypes that are present in hippocampal membranes. Therefore, the individual points are displayed without fitting. (**f**) Inhibition of binding of [3H]muscimol to rat hippocampal membrane GABA$_A$ receptors at 1mM BIC, CPZ and CLZ. Hippocampal membranes from five independent membrane preparations were incubated with 10nM [3H]muscimol in the presence of 1mM of displacing ligand in five independent experiments performed in duplicates each. One-way ANOVA followed by Tukey's multiple comparisons test was performed to determine statistically significant differences between BIC (n=5), LOX (n=5), CLZ (n=5) and CPZ (n=5), where *p<0.05 (for LOX data see Supplementary Figure S11). (**g**) Best consensus score binding mode of CLZ in comparison with the BIC bound 6X3S structure (Supplementary Figure S12). Blue arrows point to the positive ionizable feature.

To further investigate potential usage of the orthosteric site, [3H]muscimol displacement by CLZ and CPZ in direct comparison with BIC was performed in hippocampal membranes from rat brain. The hippocampus contains a high fraction of $\alpha5$-containing receptors[40,41] (Figure 6e). Near complete displacement by BIC was observed, as expected (Figure 6e). As has been observed previously in cerebellar and forebrain membranes[24], CLZ incompletely displaces the radioligand. At 1mM we see 46% displacement by CLZ and none by CPZ (Figure 6f). Similar experiments with LOX elicit 71% [3H]muscimol displacement at 1mM (Supplementary Figure S11). The lack of displacement by CPZ confirms that it does not inhibit currents via the orthosteric site of $\alpha5\beta3\gamma2$ receptors. In contrast, the displacement by CLZ further supports an orthosteric inhibition as suggested by the GABA concentration-dependent degree of inhibition. Computational docking of CLZ results in a top ranked candidate binding mode, which features the positive ionizable group in the same region of the BIC binding site as is observed for the BIC bound $\beta2/\alpha1$ interface (Figure 6g, Supplementary Figure S12). Thus, the accumulated evidence from the functional and mutational data, the muscimol displacement experiments, pharmacophore screening and computational docking indicate that CLZ inhibits GABA currents in $\alpha5\beta3\gamma2$ receptors by orthosteric inhibition, while CPZ elicits a similar degree of current inhibition by an allosteric mechanism, which is fully or partly mediated by a novel intrasubunit pocket.

Discussion

Antipsychotics have been shown to exert functional inhibition of GABA$_A$ receptors, with CLZ being the most studied compound. Previous studies noted incomplete [3H]muscimol displacement and a partly biphasic modulation of [35S]TBPS binding[14,24], pointing to a complex mode of action. This was further corroborated by additivity studies, in which CLZ was co-applied with other antipsychotics[14]. Among the drugs tested together with CLZ were LOX and CLOT, both of which had a significantly additive effect when co-applied with CLZ compared to the effect of CLZ alone. This is suggesting action on either distinctive subtypes, or different binding sites. These historical studies were methodologically heterogeneous, and subtype specific data remained scarce[13,14,21-23,26,42].

Hippocampal $\alpha5$-containing receptors are considered an emerging target for the treatment of cognitive dysfunction in schizophrenia and other neuropsychiatric conditions[6], prompting us to investigate CLZ and related compounds in this subtype. The tested compounds exert inhibitory effects on sub-saturating GABA in $\alpha5\beta3\gamma2$ receptors, with 100μM test compound eliciting current reduction ranging from -21% (IMI) to -85% (LOX and CLOT). Interactions of all compounds with GABA$_A$ receptors, with the exception of LEVO, were previously noted, but the binding sites remained elusive[13,14,24,25,43,44]. Available structural data combined with our computational analysis suggested possible involvement of the orthosteric site, and a novel allosteric site which has been described as a CPZ site in the

ECD of ELIC[27]. We thus employed mutational analysis to probe the existence of an intrasubunit "CPZ pocket" in $\alpha 5$ subunits suggested by homology with ELIC[27]. In total, we find the pharmacophore group comprising CPZ, LEVO, NOR and IMI to be responsive to the introduced mutants and for CPZ right shifts were observed. CLZ, LOX and CLOT are insensitive to the mutants. These findings together suggest that the employed mutants are a specific probe and that the site likely exists. However, mutagenesis in a protein region shared by two non-overlapping binding sites (Supplementary Figure S6) is liable to be inconclusive. Further studies with direct structural methods thus seem warranted to further clarify the usage of binding sites by CPZ and other related molecules, as mutational analysis cannot serve as definite proof.

We then complemented our functional study with radioligand displacement experiments in hippocampal membranes. At 1mM, CPZ failed to displace the standard GABA site ligand [3H]muscimol, while LOX and CLZ displaced 71 and 46%, respectively (Figure 6f, Supplementary Figure S11). For CLZ, the combination of functional and displacement data is fully consistent with orthosteric inhibition of $\alpha 5 \beta 3 \gamma 2$ receptors. Cumulative evidence from the pharmacophore models and the experimental data suggests that this is also the case for CLOT and LOX. Thus, the ligands we investigated here fall into two distinct groups, one acting as orthosteric antagonists, and the other as allosteric negative modulators. In contrast to BIC, CLZ appears to be a rather selective orthosteric antagonist that interacts with specific subtypes only (see Supplementary Figure S6 for subtype differences in the orthosteric pocket)[45].

The body of functional data we present here is intriguingly consistent with all previous data which points at a multiplicity of partly orthosteric and partly allosteric binding sites that are used differentially by molecules with tricyclic cores. We observe no functional inhibition by IMI and NOR in the most abundant receptor subtype ($\alpha 1 \beta 3 \gamma 2$; Figure 2d). The studies by Squires and Saederup did not examine current modulation, but the modulation of GABA inhibition of [35S]TBPS binding[14], which is a very sensitive indicator for interactions with ortho- and allosteric binding sites. Their work also found IMI and NOR nearly inactive[13]. We and others[14,24] observed that CLZ displaces [3H]muscimol in different brain regions to variable degrees, but never completely, indicative of orthosteric binding only at some subtypes. The additive effects in the [35S]TBPS modulation[14,23] and the biphasic effects in the study by Korpi et al are highly indicative of an allosteric component. Our data strongly suggests an orthosteric inhibition in $\alpha 5 \beta 3$ containing receptors, while the lacking inhibition in $\alpha 3 \beta 3$ suggests an unusual subtype dependency. Future studies will be needed to determine precisely the binding sites and net effects of such molecules in individual subtypes to disentangle their potential contributions to GABA$_A$ receptor mediated wanted and unwanted effects.

It is a long standing debate whether CLZ exerts part of its therapeutic effects by a GABA-ergic mechanism of action. Plasma concentrations of CLZ can reach 3 to 4μM in patients with schizophrenia[22,46]. Consistent with results showing that the elimination half-life of antipsychotics is several times greater in the human brain than in plasma[47], a study in rats shows that the concentration of CLZ can be 24-fold higher in the brain compared to the plasma concentrations[22]. Therefore, the therapeutic concentrations of CLZ in the brain can be in the high micromolar range, which would make the concentrations used in this study physiologically relevant. For CLZ and many other antipsychotics, high doses are needed to produce a therapeutic effect[22,48]. It was already questioned by Squires and Saederup in the nineties[22] if these high doses are consistent with their antipsychotic effects by means of dopamine or serotonin, for which Ki values are in the low nanomolar range[16].

Converging evidence points to pivotal alterations of GABA-ergic signaling in schizophrenia[5,6,49], and effectiveness of the benzodiazepine site ligand bretazenil as antipsychotic monotherapy[50] can be interpreted as historical support for the notion that antipsychotic action can be mediated by GABA$_A$ receptors. The role of hippocampal $\alpha 5$ subunits in multiple aspects of memory and cognitive performance has led to the development and subsequent clinical trial of basmisanil. This compound, previously known as RG-1662 or RO5186582, is an allosteric negative modulator of

$\alpha5\beta\gamma2$ receptors and has been under evaluation as an adjunctive therapy in a schizophrenic cohort for the treatment of cognitive impairment associated with schizophrenia. Very intriguingly, the functional inhibition of $\alpha5$-containing receptors we observe is much stronger for the antipsychotic compounds (CLZ, LOX and CLOT) and relatively weak for the antidepressants NOR and IMI, or LEVO (Figure 2d), which in spite of its canonical classification, does not act as an antipsychotic drug[48].

Accumulated evidence suggests a complex, likely multicausal etiology of the pathogenic mechanisms that drive schizophrenia symptoms, involving several neurotransmitter systems including dopamine, GABA and glutamate[49]. The question thus might not be whether the GABA-ergic or the dopaminergic system should best be targeted to treat schizophrenia symptoms, but which components of multiple transmitter systems should be targeted in combination for the best results. This is reflected by the notion to combine standard antipsychotic therapy with GABA-ergic "cognition enhancers", and could potentially be accomplished by compounds with an appropriate polypharmacological profile. Antipsychotic drugs and also many antidepressants display very pronounced polypharmacology. Existing data on our seven tested compounds as reflected in DrugCentral is summarized in Supplementary Figure S13. In terms of their clinical use, the seven compounds can be grouped into the antipsychotics LOX, CLOT, CLZ and CPZ. LEVO, though considered an antipsychotic, is mainly used for its strong sedative effects, while IMI and NOR are tricyclic antidepressants. In line with the high similarity among these compounds in chemical space, their molecular target profiles overlap broadly with no clear signature that would set the antidepressants apart from the antipsychotics. While still limited to seven compounds, this study suggests that effects at specific GABA$_A$ receptor isoforms might separate these two drug classes.

In conclusion, existing evidence suggests a "therapeutic portfolio" mode of action of antipsychotic medications. The exact configuration of an antipsychotic target portfolio remains to be elucidated and likely will contain both metabotropic and ionotropic receptors (Supplementary Figure S13, Supplementary Tables S8, S9). Hippocampal $\alpha5$-containing GABA$_A$ receptors are strong candidates, and strongly inhibited by the antipsychotics we tested. Molecules which hit "classical" targets such as D2 receptors and GABA$_A$ receptors may thus be an attractive alternative to the strategy that drove the development of basmisanil, namely to augment antipsychotics with GABA-ergics. Our observation that the degree of functional inhibition we observe *in vitro* appears to correlate with antipsychotic efficacy is very exciting, but definitely requires systematic investigation with a larger number of compounds and with additional methods in order to substantiate a link between their GABA$_A$ receptor effects and their therapeutic benefits. The findings of this study further emphasize the need to identify and characterize allosteric sites which may potentially be targeted and prove useful to avoid the toxicological effects associated with the orthosteric site.

Materials

Xenopus laevis oocytes were commercially purchased from Ecocyte Biosciences. Compounds purchased from Sigma Aldrich were: GABA (A2129-100g), Chlorpromazine (C8138-5g), Imipramine (I7379-5g) and Loxapine (L106-100mg), from Biomedica Medizinprodukte: Clozapine (RD 0444/50), from THP Medical products: Levomepromazine (MCE-HY-B1693-100mg), Nortriptyline (T1327-200mg), from Szabo-Scandic Handels: Clothiapine (SACSC-200404A). [3H]muscimol (NET574250UC) was purchased from PerkinElmer. All other chemicals were purchased from Sigma Aldrich.

Methods

Functional Testing with Two Electrode Voltage Clamp (TEV) in *Xenopus laevis* Oocytes

Stock solution and buffers were prepared as described in Simeone et al[51]. For the electrophysiological experiments, GABA was dissolved in NDE buffer [96 mM NaCl, 5 mM HEPES-NaOH (pH 7.5), 2 mM KCl, 1 mM $MgCl_2$, 1.8 mM $CaCl_2$] with a concentration in order to achieve the appropriate EC concentration relevant to each experiment. In brief, all other compounds were dissolved in DMSO with a stock concentration of 100mM (except CLOT in 25mM) and for further dilutions, the compounds were diluted in NDE plus GABA (EC_X).

The mutated rat $\alpha5$ GABA$_A$ receptor subunit cDNA constructs were purchased from Eurofins Genomics. The company performed the cloning by the use of site directed mutagenesis on a rat $\alpha5$ insert in a pCI vector which was provided by us. The following constructs were created: $\alpha5F53W$, $\alpha5S189W$, $\alpha5L196W$, $\alpha5L222W$ and $\alpha5F53W;L222W$ (numbering without signal peptide) and were validated by double stranded DNA sequencing. One of those (Leu196, with the equivalent Ile in ELIC) was also mutated by Nys et al and was found to cause a significant reduction in the response of GABA and no significant change in EC50[27].

In order to generate mRNA, all constructs were linearized, transcribed and purified as described previously[51]. For the microinjection, the RNA of $\alpha\beta$ receptor combinations was mixed at 1:1 ratio and $\alpha1,2\beta\gamma$ receptors were mixed at 1:1:5 ratio, whereas $\alpha5\beta\gamma$ receptors were mixed at 3:1:5 ratio ($\gamma2S$ variant). The approach used for subunit concatenation of $\alpha1\beta3\gamma2$ GABA$_A$ receptors has been described previously[35]. The dual ($\gamma2\beta3$) and triple ($\alpha1\beta3\alpha1$) constructs were injected at a ratio of 1:1[35]. $\beta2\gamma2$ receptors were mixed with a 1:3 ratio, as described in Wongsamitkul et al[30]. The RNA for the $\alpha5(mut)\beta3\gamma2$ receptor was mixed at 3:1:5 ratio, as for the wild-type $\alpha5\beta3\gamma2$, with a final concentration of 70 ng/µl.

Healthy defolliculated oocytes were injected with an aqueous solution of mRNA with a Nanoject II (Drummond). The injected oocytes were incubated at 18 °C (ND96 + antibiotic) for 2-3 days for $\alpha\beta$ receptors and for 3-4 days for $\alpha\beta\gamma$ receptors before recording. Electrophysiological recordings were performed as specified in Simeone et al[51]. A GABA concentration amounting to 5–10% of maximum GABA currents is termed EC_{5-10} (accordingly 20-30% of maximum GABA currents is EC_{20-30}, 15-30% of maximum GABA currents is EC_{15-30} etc.). All GABA concentrations used in the various experiments of this study are summarized in Supplementary Table S10. In the major receptor isoform[52] we successfully reproduced inhibitory effects on $\alpha1\beta2\gamma2$ receptors at 100µM CLZ (Figure 1a)[44]. In Figure 1b, experiments with the neurosteroid THDOC were performed, with pre-application of CLZ right before CLZ and THDOC co-application (Figure 1b). To ensure the incorporation of the $\gamma2$ subunit, diazepam was applied at the end of each measurement (~200% at 1µM). For $\beta2\gamma2$ receptors sufficient positive modulation by 50µM etomidate was used a control[30]. All recordings were performed at room temperature at a holding potential of −60 mV using a Dagan TEV-200A two-electrode voltage clamp (Dagan Corporation) and a Turbo Tec-03X npi amplifier.

Preparation of rat hippocampal membranes

51 female rats (3-4 weeks old) were sacrificed by decapitation, the 102 hippocampi removed quickly, flash frozen in liquid nitrogen and stored at -80°C until needed. Ethical review and approval was not required because the EU directive 210/63/EU, which is also reflected by the Austrian federal law „Tierversuchsgesetz 2012", states that sacrificing of animals solely for the use of their organs and tissues is not considered a "procedure" and does not require specific approval. In six independent preparations 15-18 hippocampi were homogenized with an Ultra-Turrax rotor-stator homogenizer for 30 seconds in ice-cold homogenization buffer (10 mM Hepes, 1 mM EDTA, 300 mM Sucrose) and centrifuged at 45 000 g at 4°C for 30 min. The pellet was resuspended in wash buffer (10 mM Hepes, 1 mM EDTA), incubated on ice for 30 min and centrifuged at 45 000 g at 4°C for 30 min. The pellet was stored at -80°C

o/n and the next day washed three times by suspension in 50mM Tris-citrate buffer, pH=7.1 and subsequent centrifugation as described above. Membrane pellets were stored at -80°C until final use.

Radioligand membrane displacement assays

Frozen membranes were thawed, resuspended and incubated for 60 min at 4°C in a total of 500 µl of TC50/NaCl (50 mM Tris-Citrate pH=7.1; 150 mM NaCl), various concentrations of the drug to be studied and 10 nM [3H]muscimol in the absence or presence of 10 mM GABA (to determine unspecific binding; final DMSO-concentration 1%). Membranes were filtered through Whatman GF/B filters and the filters were rinsed twice with 4 ml of ice-cold 50mM Tris/citrate buffer. Filters were transferred to scintillation vials and subjected to scintillation counting after the addition of 3ml Rotiszint Eco plus liquid scintillation cocktail. The scintillation counter used is TriCarb 4910TR from Perkin Elmer.

The individual data points were performed in duplicates and repeated in three independent experiments. For the comparison of the degree of ligand displacement at 1mM, 5 independent measurements were performed in duplicates each.

Ligand Similarity Analysis, Pharmacophore Modeling and Screening

For every ligand a conformer ensemble was generated using OMEGA 3.1.1.2 (OpenEye Scientific Software, Santa Fe, NM, USA. http://www.eyesopen.com)[53] applying default settings for all parameters and output in SD-format. Shape and color similarity scores were calculated using ROCS 3.3.1.2 (OpenEye Scientific Software, Santa Fe, NM, USA. http://www.eyesopen.com.)[32] with the -mcquery parameter set to true and applying default settings for all other parameters. The same combined multi-conf. SD-file of all ligands was specified both as input file for the query structures and the screened molecule database. The pairwise Shape Tanimoto, Color Tanimoto and Tanimoto Combo scores calculated for a particular ligand were then extracted from the corresponding ROCS CSV output file that was generated for this ligand. Hierarchical clustering was performed by means of a small python script using the clustering functionality provided by SciPy[54]. For plotting the dendrogram the Matplotlib package was used[55]. 2D scatter plots were generated in python using the multidimensional scaling (MDS) functionality provided by Scikit-learn[56]. The points, each representing one of the seven compounds, were coloured according to cluster membership and visualized by means of Matplotlib.

Ligand-based pharmacophore models of the identified ligand clusters were generated using LigandScout 4.4 (Inte:Ligand GmbH, Vienna, Austria. http://www.inteligand.com/ligandscout)[33,34]. In the ligand-based modeling perspective, all ligands constituting a cluster were added to the training-set and then conformers were generated using iCon[57] in FAST mode but with the RMSD threshold set to 0.35 to obtain denser conformer ensembles. Ligand-based model generation was performed with the output pharmacophore type set to 'Shared feature pharmacophore' and default settings for all other parameters.

Structure-based 3D pharmacophore modeling and subsequent screening of CLZ, IMI, CLO, NOR, LEVO and LOX has been performed using LigandScout 4.4. The compound pharmacophore screening database was generated using the idbgen module in LigandScout employing the 'Best' mode for conformer ensemble generation. Structure-based pharmacophores were generated from the complexes 6HUG (picrotoxin site), 6X3S (bicuculline site) and 5LG3 (CPZ bound ELIC) using LigandScout default settings in the structure-based perspective. In the screening perspective, two

screening runs with different stringency levels were carried out for each pharmacophore: a) all query features have to be matched and b) one arbitrary query feature may be omitted for hit identification. In both screening runs exclusion volume checks were enabled and the default scoring function "Pharmacophore-Fit" was used.

Computational Modeling and Docking

Alignments were generated with MOE and Promals3D. Files from the PDB (5LG3, 6A96)[27,39] were analyzed as follows: Structural superpositions were performed with the PDBeFold webserver (http://www.ebi.ac.uk/msd-srv/ssm/) and further processed with MOE (http://www.chemcomp.com). Pocket volumes were calculated with Conolly, as implemented in MOE.

Molecular Docking was performed using GOLD 5.7.167 (CPZ), and GOLD 2020.2.0 (CLZ) after appropriate preparation of protein and ligands. The ligands Ring-NR1R2 was set flexible for all docking runs. MarvinSketch 19.9 with the protonation pKa function was used to prepare the ligand species for physiological pH (one for CPZ, two for CLZ, see supplementary Figure S12).

6A96 was used as the wild type structure, and the mutants were introduced individually without further modifications using the MOE Protein Builder function. CPZ was docked into the site deduced from 5LG3: The centroid of the binding site for CPZ was chosen by the position of the sulfur from the CPZ of 5LG3 after it was superposed with the α5 subunit of 6A96. The binding site radius was set to 10Å for both binding sites.

For the CLZ docking into the orthosteric site, the centroid of the binding site was chosen by the position of the nitrogen of the BIC of 6X3S after it was superposed with the β3 and α5 interface of 6A96.

On the protein, for the CPZ docking soft potentials have been set on the residues G187-H195 (segment F) in 6A96 and the sidechains (α5V50, α5F53W, α5V56, α5V184, α5S189, α5L191, α5Y194, α5L196, α5F220 and α5L222W) were set flexible. For the CLZ docking, soft potentials have been set on the residues β3V199-A204 (loop C) in 6A96 and the side chains α5D47, α5Y49, α5F68, α5R70, α5L121, α5L131, β3T133, β3Y157, β3F200 and β3Y205 were set flexible.

For CPZ, two docking runs were performed, one with maximum diversity posing enforced for which 100 poses have been generated and one with default posing for which 300 poses were retained. For each protonation state of CLZ, 300 poses were generated with maximum diversity posing enforced. In each run Goldscore (CPZ) or CHEMPLP (CLZ) was used as the primary scoring function (default), and Chemscore for rescoring. The posing space from the diversity enforced runs was analyzed based on the top 10 solutions of either scoring function, and related poses were clustered and pooled from both runs for CPZ. Consensus score filtering led to three clusters of CPZ poses in the top three positions. Representative poses of these clusters were subjected to energy minimization with MOE and depicted to visually analyze the impact of the mutants. For CLZ, a single run per protonation state with 300 poses each led to a sufficiently converged posing space, and the binding mode poses which share features with the BIC bound state were energy minimized with MOE with the Amber10:EHT forcefield. The best ranked pose was visualized (see Supplementary Figure S12 for consensus scoring summary).

Data analysis and Figure generation

The data and statistical analysis comply with the recommendations of the *British Journal of Pharmacology* on experimental design and analysis in pharmacology[58]. TEVC data was recorded and digitized using an Axon Digidata

1550 (and Axon Digidata 1550A) low-noise data acquisition system (Axon Instruments). Data acquisition was performed using pCLAMP v.10.5 (Molecular Devices™). The same programme was used for the processing of representative traces, which were later imported to GraphPad Prism (v.6.) and visualized. A fraction of traces was analyzed in a blinded fashion. Data were analysed using GraphPad Prism (v.6.) and plotted as concentration-response curves or column graphs, as defined in Simeone et al[51]. Figures of concentration-response curves and column graphs were generated using GraphPad Prism (v.6.). These curves were normalized and fitted by non-linear regression analysis to the equation $Y = bottom + (top-bottom)/(1+(IC50/X)^{nH})$, where IC50 is the concentration of the compound that decreases the amplitude of the GABA-evoked current by 50%, and nH is the Hill coefficient. Dose response curves that do not reach saturation or where fits were not possible, were fitted by non-linear regression using constrained fits of bottom to 0 or of Hill slope to 1 for best description of the data. The fit and constraint chosen is described in the figure legends.

Structural images were generated using MOE, while images with pharmacophore models using LigandScout 4.4.

Statistics

The assumption of normality around reported mean values was confirmed using the Shapiro-Wilk test with an alpha value of 0.05. To determine the significance in variance of the results obtained from 3 or more groups, one-way ANOVA with Geisser-Greenhouse correction was performed followed by a Dunnett's multiple comparisons test. When the data do not assume a normal distribution, the non-parametric one-way ANOVA (Kruskal-Wallis test) was used followed by a Dunn's multiple comparisons test. All data are expressed as mean ± SEM. Differences between two groups were analyzed using a two-tailed Student's t-test. One sample t-test was performed in order to determine statistical significance of each mean response from control current (100%). The false discovery rate (FDR) for these tests was controlled and p-values were adjusted using the Bejamini-Hochberg method with a discovery rate (Q value) of 0.05 (where $^{\#}p<0.05$). A p-value less than 0.05 was considered statistically significant and only one level of statistical significance was used throughout the study, where $*p<0.05$ and $^{n.s.}p>0.05$. All statistical tests that have been used, and applied to sample sizes in the study, are indicated in the figure legends. The n number stated represents the number of single oocyte experiments. The exact n values are reported by the individual values shown in all scatter plot bar graphs, as well as in the figure legends and Supplementary Tables. All data subjected to statistical analysis have a group size of (n) ≥ 5. Statistical analysis was performed using GraphPad Prism (v.6.).

Data availability

The datasets generated and/or analyzed during the current study are available from the corresponding author upon request.

References

1.   Lieberman, J.A. et al. Hippocampal dysfunction in the pathophysiology of schizophrenia: a selective review and hypothesis for early detection and intervention. *Molecular Psychiatry* **23**, 1764-1772 (2018).
2.   Lodge, D.J. & Grace, A.A. Hippocampal dysregulation of dopamine system function and the pathophysiology of schizophrenia. *Trends Pharmacol Sci* **32**, 507-13 (2011).

3.   Nakahara, S., Matsumoto, M. & van Erp, T.G.M. Hippocampal subregion abnormalities in schizophrenia: A systematic review of structural and physiological imaging studies. *Neuropsychopharmacol Rep* **38**, 156-166 (2018).

4.   Skilbeck, K.J., O'Reilly, J.N., Johnston, G.A.R. & Hinton, T. The effects of antipsychotic drugs on GABAA receptor binding depend on period of drug treatment and binding site examined. *Schizophrenia research* **90**, 76-80 (2007).

5.   Marques, T.R. et al. GABA-A receptor differences in schizophrenia: a positron emission tomography study using [11C]Ro154513. *Molecular Psychiatry* (2020).

6.   Xu, M.-y. & Wong, A.H.C. GABAergic inhibitory neurons as therapeutic targets for cognitive impairment in schizophrenia. *Acta Pharmacologica Sinica* **39**, 733-753 (2018).

7.   Etherington, L.A. et al. Selective inhibition of extra-synaptic α5-GABA(A) receptors by S44819, a new therapeutic agent. *Neuropharmacology* **125**, 353-364 (2017).

8.   Gill, K.M. & Grace, A.A. The role of alpha5 GABAA receptor agonists in the treatment of cognitive deficits in schizophrenia. *Curr Pharm Des* **20**, 5069-76 (2014).

9.   Knust, H. et al. The discovery and unique pharmacological profile of RO4938581 and RO4882224 as potent and selective GABAA alpha5 inverse agonists for the treatment of cognitive dysfunction. *Bioorg Med Chem Lett* **19**, 5940-4 (2009).

10.   Sigel, E. & Ernst, M. The Benzodiazepine Binding Sites of GABAA Receptors. *Trends Pharmacol Sci* **39**, 659-671 (2018).

11.   Atack, J.R. et al. L-655,708 enhances cognition in rats but is not proconvulsant at a dose selective for alpha5-containing GABAA receptors. *Neuropharmacology* **51**, 1023-9 (2006).

12.   Glykys, J., Mann, E.O. & Mody, I. Which GABA(A) receptor subunits are necessary for tonic inhibition in the hippocampus? *J Neurosci* **28**, 1421-6 (2008).

13.   Squires, R.F. & Saederup, E. Antidepressants and metabolites that block GABAA receptors coupled to 35S-t-butylbicyclophosphorothionate binding sites in rat brain. *Brain Res* **441**, 15-22 (1988).

14.   Squires, R.F. & Saederup, E. Clozapine and Several Other Antipsychotic/Antidepressant Drugs Preferentially Block the Same 'Core' Fraction of GABAA Receptors. *Neurochemical Research* **23**, 1283-1290 (1998).

15.   Attard, A. & Taylor, D.M. Comparative effectiveness of atypical antipsychotics in schizophrenia: what have real-world trials taught us? *CNS Drugs* **26**, 491-508 (2012).

16.   Seeman, P. Targeting the dopamine D2 receptor in schizophrenia. *Expert Opin Ther Targets* **10**, 515-31 (2006).

17.   Mozrzymas, J.W., Barberis, A., Michalak, K. & Cherubini, E. Chlorpromazine inhibits miniature GABAergic currents by reducing the binding and by increasing the unbinding rate of GABAA receptors. *J Neurosci* **19**, 2474-88 (1999).

18.   Schwartz, R.D. & Mindlin, M.C. Inhibition of the GABA receptor-gated chloride ion channel in brain by noncompetitive inhibitors of the nicotinic receptor-gated cation channel. *J Pharmacol Exp Ther* **244**, 963-70 (1988).

19.   Seeman, P. Brain dopamine receptors. *Pharmacol Rev* **32**, 229-313 (1980).

20.   Yokota, K. et al. The effects of neuroleptics on the GABA-induced Cl- current in rat dorsal root ganglion neurons: differences between some neuroleptics. *Br J Pharmacol* **135**, 1547-55 (2002).

21.   Squires, R.F. & Saederup, E. Mono N-aryl ethylenediamine and piperazine derivatives are GABAA receptor blockers: implications for psychiatry. *Neurochem Res* **18**, 787-93 (1993).

22.   Squires, R.F. & Saederup, E. Clozapine and some other antipsychotic drugs may preferentially block the same subset of GABA(A) receptors. *Neurochem Res* **22**, 151-62 (1997).

23.   Squires, R.F. & Saederup, E. Additivities of compounds that increase the numbers of high affinity [3H]muscimol binding sites by different amounts define more than 9 GABA(A) receptor

complexes in rat forebrain: implications for schizophrenia and clozapine research. *Neurochem Res* **25**, 1587-601 (2000).

24. Korpi, E.R., Wong, G. & Luddens, H. Subtype specificity of gamma-aminobutyric acid type A receptor antagonism by clozapine. *Naunyn Schmiedebergs Arch Pharmacol* **352**, 365-73 (1995).

25. Michel, F.J. & Trudeau, L.E. Clozapine inhibits synaptic transmission at GABAergic synapses established by ventral tegmental area neurones in culture. *Neuropharmacology* **39**, 1536-43 (2000).

26. Squires, R.F. & Saederup, E. Clozapine's antipsychotic effects do not depend on blockade of 5-HT3 receptors. *Neurochem Res* **24**, 659-67 (1999).

27. Nys, M. et al. Allosteric binding site in a Cys-loop receptor ligand-binding domain unveiled in the crystal structure of ELIC in complex with chlorpromazine. *Proc Natl Acad Sci U S A* **113**, E6696-e6703 (2016).

28. Wohlfarth, K.M., Bianchi, M.T. & Macdonald, R.L. Enhanced neurosteroid potentiation of ternary GABA(A) receptors containing the delta subunit. *J Neurosci* **22**, 1541-9 (2002).

29. Puia, G. et al. Neurosteroids act on recombinant human GABAA receptors. *Neuron* **4**, 759-65 (1990).

30. Wongsamitkul, N. et al. α subunits in GABA(A) receptors are dispensable for GABA and diazepam action. *Sci Rep* **7**, 15498 (2017).

31. Squires, R.F. & Saederup, E. GABAA receptor blockers reverse the inhibitory effect of GABA on brain-specific [35S]TBPS binding. *Brain Res* **414**, 357-64 (1987).

32. Hawkins, P.C.D., Skillman, A.G. & Nicholls, A. Comparison of Shape-Matching and Docking as Virtual Screening Tools. *Journal of Medicinal Chemistry* **50**, 74-82 (2007).

33. Wolber, G., Dornhofer, A.A. & Langer, T. Efficient overlay of small organic molecules using 3D pharmacophores. *J Comput Aided Mol Des* **20**, 773-88 (2006).

34. Wolber, G. & Langer, T. LigandScout: 3-D pharmacophores derived from protein-bound ligands and their use as virtual screening filters. *J Chem Inf Model* **45**, 160-9 (2005).

35. Simeone, X. et al. Defined concatenated α6α1β3γ2 GABA(A) receptor constructs reveal dual action of pyrazoloquinolinone allosteric modulators. *Bioorg Med Chem* **27**, 3167-3178 (2019).

36. Kim, J.J. et al. Shared structural mechanisms of general anaesthetics and benzodiazepines. *Nature* **585**, 303-308 (2020).

37. Masiulis, S. et al. GABA(A) receptor signalling mechanisms revealed by structural pharmacology. *Nature* **565**, 454-459 (2019).

38. Puthenkalam, R. et al. Structural Studies of GABA-A receptor binding sites: Which experimental structure tells us what? *Frontiers in Molecular Neuroscience* **9**(2016).

39. Liu, S. et al. Cryo-EM structure of the human α5β3 GABA(A) receptor. *Cell Res* **28**, 958-961 (2018).

40. Pirker, S., Schwarzer, C., Wieselthaler, A., Sieghart, W. & Sperk, G. GABA(A) receptors: immunocytochemical distribution of 13 subunits in the adult rat brain. *Neuroscience* **101**, 815-50 (2000).

41. Sperk, G., Schwarzer, C., Tsunashima, K., Fuchs, K. & Sieghart, W. GABA(A) receptor subunits in the rat hippocampus I: immunocytochemical distribution of 13 subunits. *Neuroscience* **80**, 987-1000 (1997).

42. Squires, R.F. & Saederup, E. A review of evidence for GABergic predominance/glutamatergic deficit as a common etiological factor in both schizophrenia and affective psychoses: more support for a continuum hypothesis of "functional" psychosis. *Neurochem Res* **16**, 1099-111 (1991).

43. Besnard, J. et al. Automated design of ligands to polypharmacological profiles. *Nature* **492**, 215-220 (2012).

44. Asproni, B. et al. Synthesis and pharmacological evaluation of 1-[(1,2-diphenyl-1H-4-imidazolyl)methyl]-4-phenylpiperazines with clozapine-like mixed activities at dopamine D(2), serotonin, and GABA(A) receptors. *J Med Chem* **45**, 4655-68 (2002).

45. Rahman, M. et al. GABA-site antagonism and pentobarbital actions do not depend on the alpha-subunit type in the recombinant rat GABA receptor. *Acta Physiol (Oxf)* **187**, 479-88 (2006).

46. Yada, Y. et al. The relationship between plasma clozapine concentration and clinical outcome: a cross-sectional study. *Acta Psychiatr Scand* **143**, 227-237 (2021).

47. Tauscher, J., Jones, C., Remington, G., Zipursky, R.B. & Kapur, S. Significant dissociation of brain and plasma kinetics with antipsychotics. *Mol Psychiatry* **7**, 317-21 (2002).

48. Huhn, M. et al. Comparative efficacy and tolerability of 32 oral antipsychotics for the acute treatment of adults with multi-episode schizophrenia: a systematic review and network meta-analysis. *Lancet* **394**, 939-951 (2019).

49. Charych, E.I., Liu, F., Moss, S.J. & Brandon, N.J. GABA(A) receptors and their associated proteins: implications in the etiology and treatment of schizophrenia and related disorders. *Neuropharmacology* **57**, 481-95 (2009).

50. Delini-Stula, A. & Berdah-Tordjman, D. Antipsychotic effects of bretazenil, a partial benzodiazepine agonist in acute schizophrenia--a study group report. *J Psychiatr Res* **30**, 239-50 (1996).

51. Simeone, X. et al. Molecular tools for GABAA receptors: High affinity ligands for β1-containing subtypes. *Scientific Reports* **7**, 5674 (2017).

52. Olsen, R.W. & Sieghart, W. International Union of Pharmacology. LXX. Subtypes of gamma-aminobutyric acid(A) receptors: classification on the basis of subunit composition, pharmacology, and function. Update. *Pharmacol Rev* **60**, 243-60 (2008).

53. Hawkins, P.C.D., Skillman, A.G., Warren, G.L., Ellingson, B.A. & Stahl, M.T. Conformer Generation with OMEGA: Algorithm and Validation Using High Quality Structures from the Protein Databank and Cambridge Structural Database. *Journal of Chemical Information and Modeling* **50**, 572-584 (2010).

54. Virtanen, P. et al. SciPy 1.0: fundamental algorithms for scientific computing in Python. *Nature Methods* **17**, 261-272 (2020).

55. Hunter, J.D. Matplotlib: A 2D Graphics Environment. *Computing in Science & Engineering* **9**, 90-95 (2007).

56. Pedregosa, F. et al. Scikit-learn: Machine Learning in Python. *Journal of Machine Learning Research* **12**(2012).

57. Poli, G., Seidel, T. & Langer, T. Conformational Sampling of Small Molecules With iCon: Performance Assessment in Comparison With OMEGA. *Frontiers in Chemistry* **6**(2018).

58. Curtis, M.J. et al. Experimental design and analysis and their reporting II: updated and simplified guidance for authors and peer reviewers. *Br J Pharmacol* **175**, 987-993 (2018).

Acknowledgements

Author contributions

K.B., M.W. and M.E. conceived the study. K.B. planned and supervised electrophysiological experiments. K.B., L.S., S.R., F.D.V. and F.Z. performed electrophysiological measurements and data analysis. P.S. performed radioligand assays and data analysis. F.K. performed structural analysis and computational docking. T.S., A.G. and T.L. performed similarity analysis, pharmacophore modelling and screening. K.B., M.E. and M.W. wrote the manuscript. K.B., F.K. and F.Z. prepared figures.

Additional information

Supplementary information accompanies this paper.

Competing interests: The authors declare no competing interests.

Declaration of transparency and scientific rigour: This Declaration acknowledges that this paper adheres to the principles for transparent reporting and scientific rigour of preclinical research recommended by funding agencies, publishers and other organisations engaged with supporting research.